

Infrared Cavity Ringdown Spectroscopy of Jet-Cooled Nucleotide Base Clusters and Water Complexes

Raphael N. Casaes,[†] Joshua B. Paul,[‡] R. Patrick McLaughlin,[§] and Richard J. Saykally*[¶]

Department of Chemistry, University of California, Berkeley, California 94720-1460

Tanja van Mourik

Department of Chemistry, University College, London, WC1H 0AJ, United Kingdom

Received: April 22, 2004

We present the first direct infrared absorption measurements of gas phase nucleotide base clusters and complexes with water. Spectra in the NH stretching region indicate the presence of several doubly H-bonded isomers of both thymine and uracil dimers, as well as both larger base clusters and uracil–water complexes, but no singly H-bonded species are observed. Three NH stretching bands are assigned to three different uracil–water dimer isomers. Bands due to larger complexes are also observed, but due to spectral congestion, assignment to specific clusters is tentative. The IR cavity ringdown laser absorption spectroscopy results show unusually large bonded OH stretch red shifts for uracil–water clusters, providing evidence of the extremely strong hydrogen bonds formed between these molecules predicted in *ab initio* calculations.

Introduction

The five nucleotide bases (adenine, guanine, thymine, cytosine, and uracil) found in DNA and RNA govern the replication of DNA, store information required to synthesize proteins, and are responsible for the transcription of this information to the ribosome where proteins are synthesized. In the Watson–Crick model of DNA, the purines (adenine (A) and guanine (G)) form strong hydrogen bonds to the pyrimidines, cytosine (C) and thymine (T) as A–T and C–G base pairs, whereas in RNA uracil (U) replaces thymine. Both DNA replication and protein synthesis, wherein a segment of the DNA double helix is “unzipped” and new complementary strands are constructed on the unraveled strands, involve the breaking of these hydrogen bonds. During these base pair opening processes, water molecules can interact with nucleotide bases through major and minor grooves in the helix.¹ Clearly, a detailed understanding of the hydrogen bonding interactions between the nucleotide bases and between nucleotide bases and water is essential for modeling the behavior of nucleic acids in solution.

Several theoretical studies of uracil clusters have appeared in the recent literature.^{2–5} Kratochvil et al. conducted an exhaustive search of the dimer potential energy surface using the quenching/molecular dynamics/AMBER 4.1 method followed by optimization of the minimum energy structures at the HF/6-31G** and MP2 levels.³ The authors found 11 low-energy minima structures located on the potential energy surface of the uracil dimer: 7 hydrogen bonded (closed structures wherein two hydrogen bonds are formed between the molecules), 1 T-shaped structure, and 3 stacked structures, wherein the interaction energy is dominated by dispersion.

Mixed uracil–water clusters have been the subject of numerous theoretical studies.^{6–12,13} Gadre et al. investigated the stepwise hydration of uracil, employing an electrostatic based model (EPIC) followed by optimization at the B3LYP/6-31+G (2d,p) level of theory.⁹ By analyzing the difference in the interaction energy between uracil–water clusters and pure water clusters (ΔE_{rel}), the authors found evidence that the first hydration shell of uracil contains 6 water molecules and that ΔE_{rel} converges for clusters with 10 or more water molecules, indicating that water–water interactions are dominant for clusters of this size (i.e., additional water molecules no longer “see” the solvated uracil). Second-order Møller–Plesset perturbation theory (MP2) studies by van Mourik⁷ and Dolgounitcheva⁸ found four minima on the uracil–H₂O potential energy surface. In all four isomers, the water molecule acts as both a hydrogen bond donor and acceptor.

van Mourik and co-workers have also carried out diffusion quantum Monte Carlo (DQMC) simulations of uracil–water clusters using a distributed multipole analysis (DMA) model potential, fit to MP2 results, which correctly represents non-spherical effects due to anisotropic features of the charge distribution.¹² The authors found that all of the four uracil–H₂O minima, and the two lowest uracil–(H₂O)₂ clusters, are vibrationally stable; viz. the barrier height separating adjacent minima is high enough so that no interconversion between different minima is observed in the DQMC simulation, whereas the free water hydrogen atoms are delocalized above and below the plane. To facilitate the interpretation of the cavity ringdown laser absorption spectroscopy (CRLAS) data, we have conducted harmonic frequency calculations on several uracil–water complexes previously studied by *ab initio* and DQMC methods.

Previous vibrational spectroscopy studies have addressed the individual bases, and some base clusters, in low-temperature Ar and N₂ matrixes^{14–19} and in heated cells.²⁰ The gas-phase heated cell experiments revealed that single uracil, thymine, and adenine tautomers are present in the gas phase at temperatures

* Corresponding author. E-mail: saykally@uclink4.berkeley.edu.

[†] Current address: Lam Research Corporation, 4650 Cushing Parkway, Fremont, CA 94538.

[‡] Current address: NovaWave Technologies, 230A Twin Dolphin Drive, Redwood Shores, CA 94065.

[§] Current address: University of Washington, Seattle, WA 98195.

up to 350 °C.²⁰ Some features in the matrix isolation experiments have been assigned to uracil dimers and thymine dimers.²¹ However, Ivanov et al. have shown that analysis of the uracil matrix spectrum is complicated by matrix splittings, Fermi resonances, and changes in lattice site occupancies upon annealing.¹⁹ Graindourze et al. assigned some bands in their spectrum to an open isomer of the uracil dimer based on the splitting of the free NH stretching band upon annealing. This assignment is quite probably in error, as recent calculations on the uracil dimer potential energy surface found only one “open” minimum located 33.9 kJ/mol above the global minimum.³

The study of nucleotide bases via molecular beam methods was pioneered by Brady et al.²² Brady and co-workers found that the electronic spectrum of uracil was broad and diffuse, indicating either a strong mixing of electronic states or a large geometry change between ground and excited states. Anion photoelectron spectroscopy studies by Desfrancois and co-workers revealed that uracil and thymine stabilize the surplus electron in a dipole bound state, wherein the electron is bound by the rotating dipole moment, mostly outside the molecule.²³ The authors found that a single argon atom is sufficient to stabilize the surplus electron in the π^* LUMO valence bound state. Shiedt et al. investigated the anion photoelectron spectra of nucleotide base complexes with water,²⁴ finding that attachment of water molecules to the anion leads to a linear increase in binding energy as a function of the number of water molecules and a broadening of the photoelectron peak, indicative of valence binding. By extrapolating this binding energy dependence to zero water molecules, the authors found that the π^* LUMOs of uracil, thymine, and cytosine are situated at low and very similar energies, an ideal precondition for efficient charge transfer in DNA.

An infrared diode laser study of uracil made by Viant et al., using a heated pulsed molecular beam source developed in our lab to entrain nonvolatile samples into supersonic expansions, produced a rotationally resolved vibrational spectrum of this molecule in the carbonyl stretching region with a rotational temperature of 20 K.²⁵ Such direct absorption infrared gas phase experiments employing cold molecular beams are ideally suited for studying the hydrogen bonding interaction in small clusters of nucleotide bases or their complexes with water molecules. The cold rotational and vibrational temperatures attained in molecular beams significantly simplify the spectrum, whereas appropriate expansion conditions allow for the generation of small clusters. However, because of the spectral broadening due to vibrational predissociation that is typical of hydrogen bonded clusters, mid-infrared experiments typically do not resolve rotational or tunneling fine structure. As a result, only information on hydrogen bonding interaction strength and cooperativity, as gauged by red shifts of hydrogen bonded NH and OH stretch modes, can be extracted from these experiments. Corresponding experiments in the far-infrared region are necessary to provide dynamical information on hydrogen bond rearrangements, thus affording a detailed understanding of the intermolecular potential energy surfaces of these complexes.²⁶

Experimental Setup

The Berkeley medium resolution infrared cavity ringdown spectrometer used to obtain the results presented below has been described in recent publications.^{27,28} Briefly, tunable infrared radiation was generated by stimulated Raman scattering of a Nd:YAG pumped dye laser (30–40 mJ/pulse, 8 ns pulse width). A Herriot cell was used to achieve 17 refocused passes through 200 psi of hydrogen. This generated 0.2–0.5 mJ/pulse infrared

(2.7–3.4 μm) radiation in the third Stokes band with a 0.2 cm^{-1} bandwidth. The tunable infrared radiation was injected into the ringdown cavity, formed by two highly reflective dielectric mirrors ($R \approx 0.9999$), and the subsequent decay was monitored by a liquid nitrogen cooled InSb detector. The signal was amplified, digitized, and sent to a computer for analysis. Per pass fractional losses were derived from a least-squares fit of the signal to a single-exponential decay function and recorded as a function of wavelength.

The heated slit source utilized in these experiments was first designed by Liu et al.²⁹ and used in high-resolution IR diode laser absorption spectroscopy of uracil²⁵ and subsequent IR CRLAS studies of arginine.³⁰ The source has two compartments: a detachable oven region that holds the solid sample and a main body region containing a 4 in. slit. A plate with a series of small holes separates the two source compartments. The entire source is made of gold plated solid copper, which ensures even heating and minimizes the decomposition of nucleotide bases and amino acids.

The 4 in. pulsed slit molecular beam source is heated to 210–220 °C using two 300 W strip heaters (Omega Heating) placed on the upper and lower surfaces of the source. The top heater is kept at a slightly higher temperature to prevent condensation of the vapors in the top compartment. This source typically operates at 40 Hz with a He carrier gas backing pressure of 50–60 psi (3–4 atm). During operation, the chamber pressure was kept at 300 mTorr by a Roots pump backed by a mechanical pump. The He carrier gas is heated to 210–220 °C before entering the source as another precaution against condensation. If condensation in the top source compartment does occur, then solid particles will be introduced into the expansion increasing the noise due to scattering to unacceptable levels.

Ab Initio Calculations. We have calculated harmonic vibrational frequencies for the four uracil–water dimers reported in refs 12 and 13. The frequencies were computed at the same level of theory (MP2/DZPi) as used to fully optimize the geometries. Interaction energies (D_e) are computed at the same level of theory as well.

DZPi is an “interaction-optimized” basis set; the exponents of the polarization functions were obtained by optimizing the interaction energy contributions of selected small van der Waals complexes.¹ MP2 calculations on indole water indicate that DZPi yields interaction energies for standard hydrogen-bonded systems comparable to those obtained with the much larger aug-cc-pVDZ basis set.²

Harmonic vibrational frequencies are not well-suited for comparison to experimental frequencies, as the anharmonicity contribution to the frequencies may be large. One of the principal methods for calculating anharmonic vibrational frequencies is the vibrational self-consistent field (VSCF) method (and its correlation-corrected form, CC-VSCF), of which the basic concept was introduced in 1978.³ However, although efficient variations of this method are being developed,^{4,5} current implementations of the CC-VSCF method are not yet routinely applicable to molecular systems of the size as those studied in the current paper. Another way to account for anharmonicity is the use of scaling factors.⁶ Choosing a suitable scaling factor is however not straightforward, as the optimal scaling factor may depend on the particular vibrational mode, the method and basis set used, as well as the type of molecular system studied. A recent study by Schoone et al.⁷ showed some correlation between the optimal scaling factor (taken as the ratio of the experimental and theoretical water OH stretch frequency) and

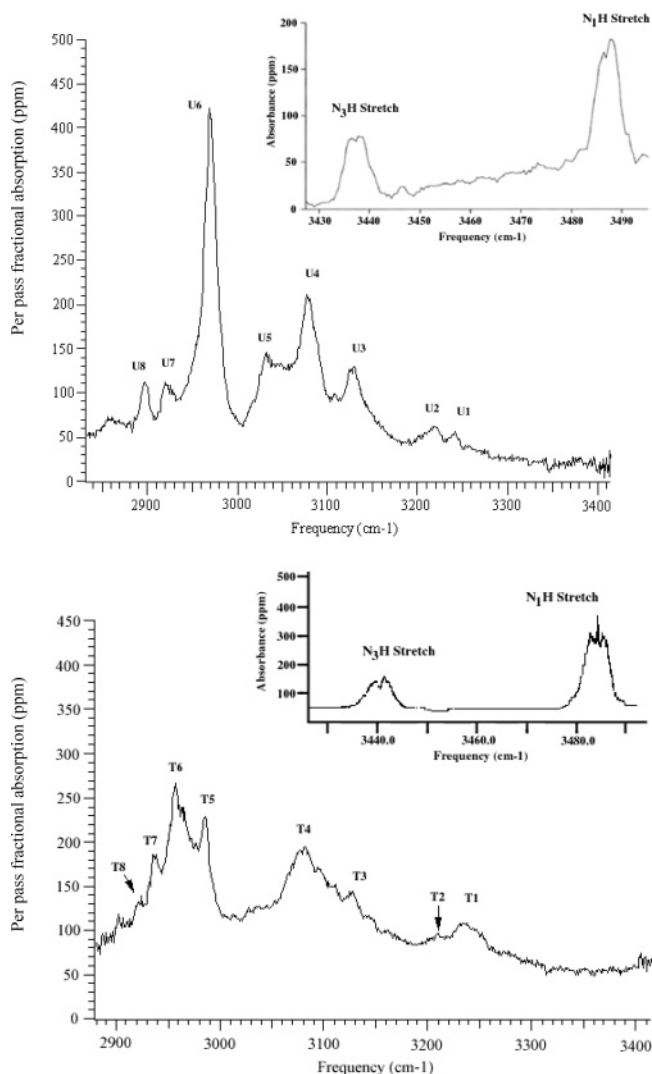


Figure 1. IR-CRLAS spectra of the N–H stretching regions of gas-phase uracil (top) and thymine (bottom). Insets show monomer NH stretch bands whereas the main graphs show red shifted NH stretch bands (U1–8 and T1–8) due to clusters.

TABLE 1: Comparison of Uracil and Thymine Band Positions from IR-CRLAS Experiments and Argon Matrix Experiments^a

uracil			thymine		
band	CRLAS	Ar matrix	band	CRLAS	Ar matrix
Monomer					
N1H	3486.3	3485	N1H	3484.9	3480
N3H	3437.7	3435	N3H	3439.4	3434
Dimer					
U1	3240.1	3215	T1	3236.4	3225
U2	3218.3	3185	T2	3208.5	3184
Larger Clusters					
U3	3127.5	3115	T3	3125.6	3130
U4	3077.4	3060	T4	3078.3	3079
U5	3032.2		T5	2985.2	
U6	2968		T6	2958.5	
U7	2944.3		T7	2937.4	
U8	2920.1		T8	2919.2	

^a Assignments shown here do not necessarily correspond to assignments given in ref 17.

the interaction energy for 1:1 hydrogen-bonded complexes of water and pyridine or imidazole derivatives. For these complexes, the optimal scaling factor slightly decreases with increasing interaction energy. However, for closed X···H–O···

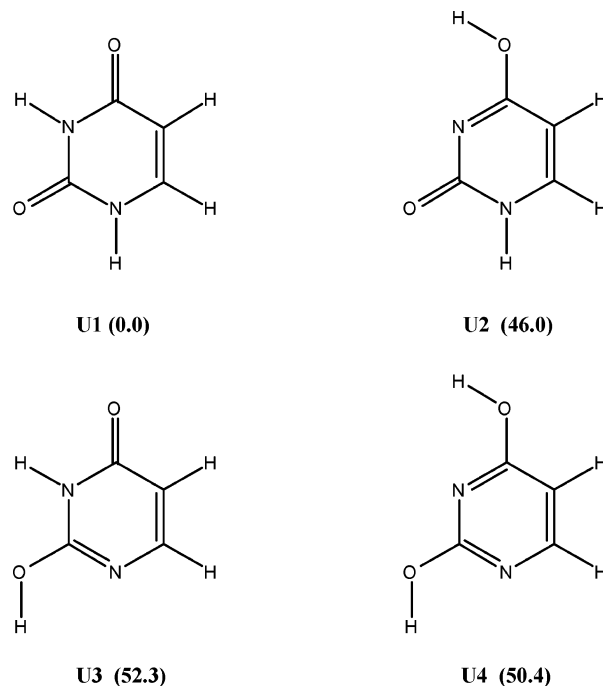


Figure 2. The four most energetically stable tautomeric structures of uracil.

H–N (X = N, O, or S) hydrogen-bonded complexes with water, which exhibit hydrogen-bond patterns comparable to those in uracil–water, this correlation is absent.⁸ Instead, a comparison of the experimental and computed OH or NH stretch frequencies reveals an approximately linear relationship between the experimental and theoretical values,⁸ indicating that the application of a uniform scaling factor to account for anharmonicity is reasonable in this case. The optimal scaling factor appeared to be slightly smaller for the NH than that for the OH stretches in the C=O···H–O···H–N hydrogen-bonded systems studied in ref 8. As we found that a scaling factor of 0.98 gave MP2 frequencies in very good agreement with experiment for hydrogen-bonded OH stretches in noradrenaline,⁹ we have used scaling factors of 0.98 and 0.97 to scale down the uracil–water OH and NH stretches, respectively.

Uracil and Thymine Monomers and Clusters. About 5.0 g of uracil (or thymine) was placed into the sample compartment of the oven source and heated to 210 °C. Fourier transform infrared (FTIR) spectra of uracil and thymine samples condensed onto glass slides following expansion from the source showed no change when compared to FTIR spectra obtained from unheated samples, suggesting that minimal decomposition was occurring. Furthermore, visual inspection of the detachable sample compartment showed only slight discoloration, a result that would indicate the presence of decomposition in the remaining sample. As long as the source temperature was kept below 230 °C, no decomposition of uracil or thymine was observed. With a He carrier gas stagnation pressure of 35 psi (~2 atm) and a pulsed valve repetition rate of 40 Hz, the region from 2850 to 3500 cm⁻¹ was scanned with the IR-CRLAS spectrometer. The results of the scans for uracil and thymine are shown in Figure 1. The measured band positions for uracil and thymine in this region are summarized in Table 1 along with the corresponding band positions measured in argon matrix experiments.

The relative intensities of the two uracil NH stretch bands agree well with the intensities predicted by our MP2/DZPi calculations, 114 km/mol for the ν_1 mode and a 68 km/mol for the ν_2 mode. As shown in Figure 1, the N₃–H stretch is indeed

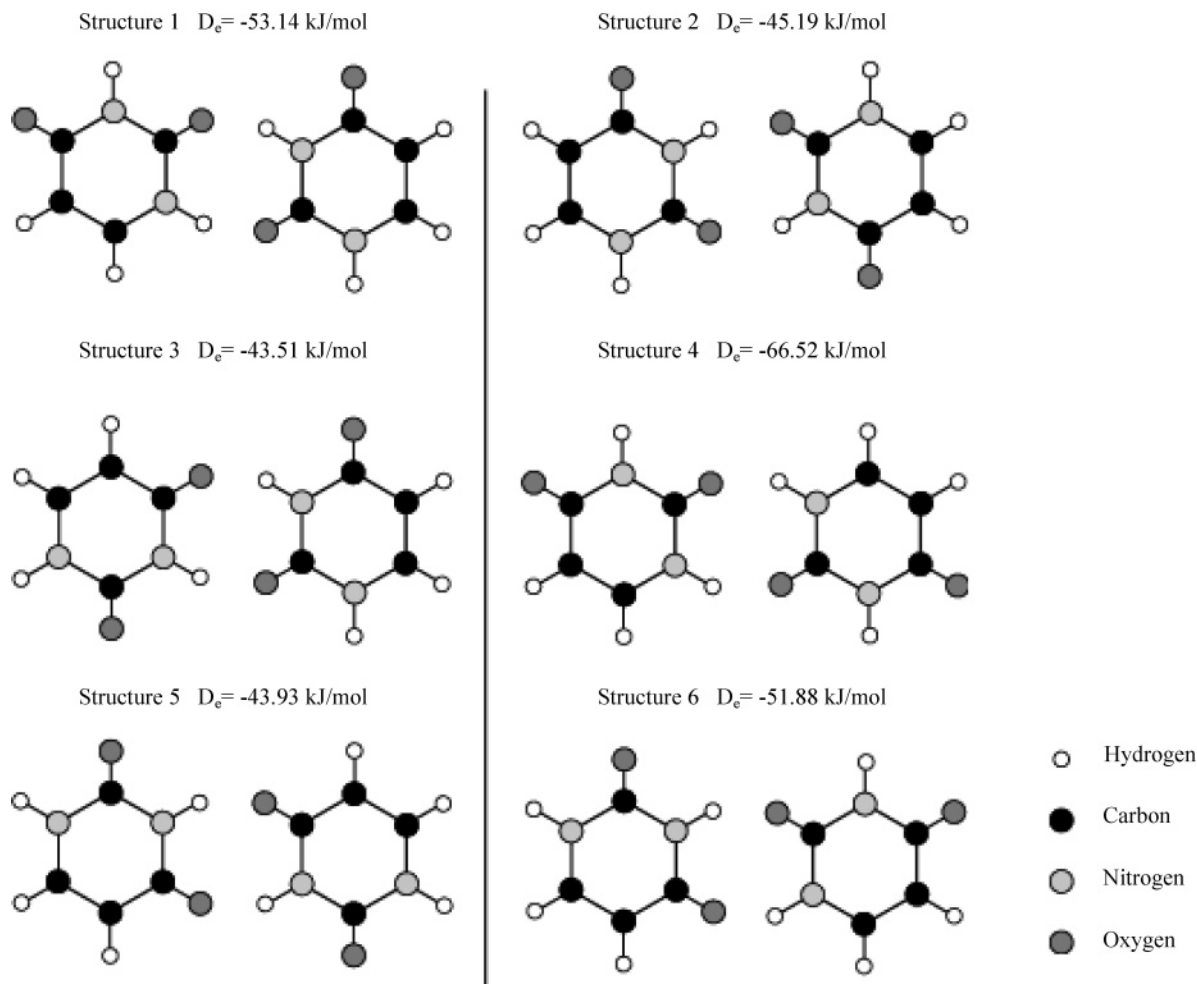


Figure 3. Six calculated low-energy uracil dimer structures from ref 2 containing two hydrogen bonds involving NH and CO groups. Four other structures, 3 stacked, 1 T-shaped, and 1 involving a CH hydrogen bond donor, are also minima in the dimer PES.

about 0.6 times the strength of the N_1-H stretch, and the same relative intensities were observed for the two thymine $N-H$ stretches. When scaled by 0.98, appropriate for this level of theory, the predicted frequencies of these two bands are 3510 and 3457 cm^{-1} , also in good agreement with the experimental results. Furthermore, the $N-H$ stretch frequencies measured in argon matrices¹⁷ agree surprisingly well with the IR-CRLAS gas-phase results.

The fact that both of the $N-H$ stretching bands were observed for uracil and thymine monomers in this region and that the intensities agree well with the theoretical values suggests that the only gas-phase tautomeric structure observed for both of these molecules in the supersonic expansion is the diketo form, in agreement with the heated cell experiments of Colarusso et al.²⁰ Of the four tautomeric structures that would reasonably be expected to exist for uracil and thymine in the molecular beam, only one, the diketo tautomer, has both the N_1-H and N_3-H stretches active (Figure 2). The other tautomeric structures for both of these molecules have one, or both, of these $N-H$ sites missing due to keto-enol tautomerization. If a considerable population of another tautomer were present in the expansion, then the relative intensities of the $N-H$ stretches would not agree as well with the calculated values.

Eight bands observed in the uracil and thymine spectra cannot be assigned to monomer transitions. The only monomer fundamental modes that could account for bands in the 3000–3300 cm^{-1} region are CH stretches. However, given the intensity of the NH stretch bands, the CH stretches are much too weak

to be observed with CRLAS. Combination bands arising from vibrationally hot monomers could also account for some of these bands. However, such combination bands are expected to have significantly lower transition strength than the fundamental transitions, although all of the observed bands are of the same order of magnitude. Furthermore, the bandwidth of these bands are approximately twice that of the monomer NH stretch bands, suggesting that the band carriers are different. Because no decomposition was observed, all of these bands must be assigned to hydrogen-bonded NH stretches of *clusters*.

As mentioned previously, Kratochvil et al. located 11 minima in the uracil dimer potential energy surface. Although the authors did not calculate the vibrational frequencies of these structures, some estimates can be made. We can certainly differentiate between the three classes of isomers, double hydrogen bond, T-shaped, and stacked, based on the magnitude of the NH stretch red shift. Of these three classes, the double hydrogen-bonded structures must display the largest NH stretch red shift because of hydrogen bond cooperativity, whereas the stacked structures must possess a minimal NH stretch shift, because there is no hydrogen bonding in these structures. Furthermore, we can differentiate between different double hydrogen-bonded structures based on the number of red shifted NH stretch bands observed. Figure 3 shows six of the seven double hydrogen-bonded structures found in the dimer potential energy surface (PES) by Hobza and co-workers. Structures 2, 4, and 7 (not shown) have only one NH stretch band whereas the other three have two. Finally, we can get a rough estimate of the red shift

based on our uracil–water calculations. These red shifts vary from 274 to 309 cm^{-1} , which would place the uracil dimer NH stretches around 3200 cm^{-1} . Given these results, we assign the two bands at 3240.1 and 3218.3 cm^{-1} to the NH stretches of a doubly hydrogen bonded form of the uracil dimer.

Although we cannot assign with certainty these bands to a particular uracil dimer isomer, we can limit the possibilities. First of all, we can assume that the calculated global minimum structure (structure 4) is present in the expansion. Structure 4 possess two identical hydrogen bonds involving the N_1H hydrogen and should display a single NH band. Because we observe two bands in the dimer NH stretch region, multiple dimer isomers must be present in the expansion. The second and third lowest energy structures (1 and 6) have both N_1H and N_3H hydrogens involved in hydrogen bonding. As the monomer N_1H stretch occurs at higher frequency than the N_3H stretch, we assign the **U1** band at 3240.1 cm^{-1} to a convolution of the N_1H hydrogen bonded stretches of structures 1, 4, and 6, and the **U2** band, at 3218.3 cm^{-1} , to a convolution of the N_3H hydrogen bonded stretches of structures 1 and 6. However, band **U2** is broader and slightly stronger than band **U1**, indicating that **U2** is due to other isomers in addition to 1 and 6. Structures 2, 3, and 5 only have the N_3H hydrogen involved in hydrogen bonding and thus are additional candidates for this band. However, we see no evidence for structure 7, T-shaped structures, or stacked structures, as we do not observe any bands to the blue of **U1** or to the red of the free NH stretch.

We are not aware of any calculations on the thymine dimer PES analogous to those of Kratochvil et al. for the uracil dimer. However, as uracil and thymine differ only by the presence of a methyl group in place of a hydrogen, it is expected that the double hydrogen-bonded thymine dimer structures are analogous to the uracil dimer structures. This is certainly reflected in the similarity of their IR-CRLAS spectra. As such, we assign bands **T1** and **T2** to hydrogen-bonded NH stretches of doubly hydrogen bonded thymine dimers. In the thymine spectra, band **T1** is significantly stronger than band **T2**, perhaps indicating a greater relative population of N_1H hydrogen-bonded structures.

Bands **U3–U8** and **T3–T8** are significantly red shifted and, in the absence of evidence for decomposition, must be assigned to clusters larger than the dimer. Unfortunately, there are no theoretical studies of uracil or thymine clusters larger than the dimer, hence a definitive assignment of these bands is not possible. In light of the uracil dimer PES study, larger clusters will also possess several low energy isomers, some of which will have significant populations in the molecular beam expansion. We can divide these bands into two regions based on the magnitude of the NH stretch red shift. Bands **U3**, **U4**, **U5**, **T3**, and **T4** are red shifted by approximately 300 to 400 cm^{-1} , whereas bands **U6**, **U7**, **U8**, **T5**, **T6**, **T7**, and **T8** are shifted by 500 to 550 cm^{-1} . This separation of bands into distinct regions is typical of hydrogen-bonded clusters and reflects an increase in hydrogen bonding cooperativity as a function of cluster size. As such, we tentatively assign the bands in the first region to trimers and those in the second region to tetramers. The general appearance of the uracil and thymine spectra is very similar, indicating that the band carriers have similar structures. The loss of band structure in the thymine spectra when compared to the uracil spectra reflects the presence of additional conformers or hot bands afforded by the presence of a methyl group. Of particular interest is the uracil band **U6** at 2986 cm^{-1} . The high intensity and small bandwidth of this band indicates the presence of a highly stable and symmetrical cluster wherein all

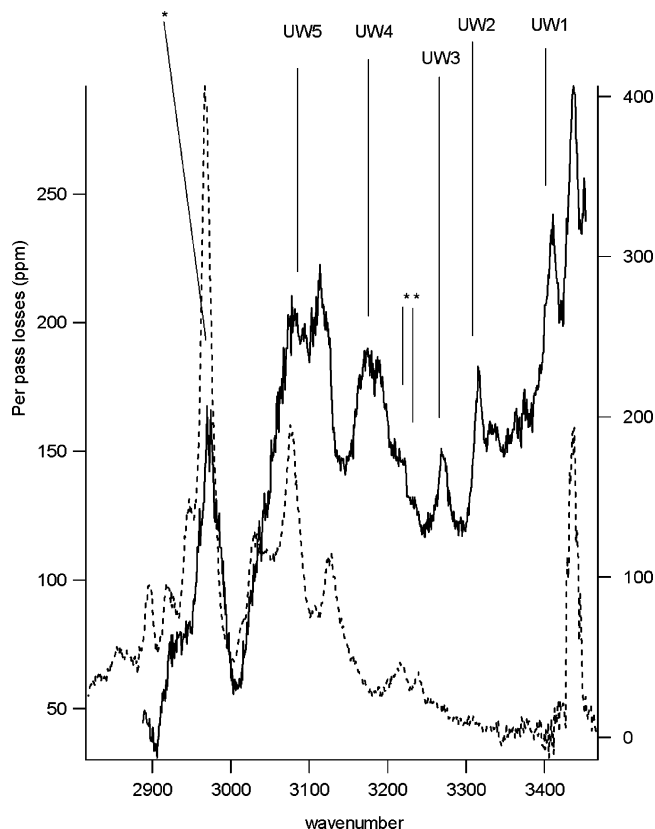


Figure 4. IR-CRLAS spectra of uracil–water (solid lines) and uracil clusters (dashed lines) in the 2900–3450 cm^{-1} region. The left y axis corresponds to the uracil–water data and the right y axis refers to the uracil cluster data. Note the appearance of three new peaks in the uracil–water spectrum, not shifted as far to the red as the uracil homodimer clusters, and two broad bands to the red of the homodimer bands.

TABLE 2: Uracil–Water Band Positions Measured via IR-CRLAS^a

band	frequency	fwhm	$\Delta_{(\text{N}_3\text{H})}$
UW1	3411.3	16.2	26.4
UW2	3316.7	15	121
UW3	3270.9	14.9	166.8
UW4	3181.9	59	255.8
UW5	3099.7	88.5	338

^a $\Delta_{(\text{N}_3\text{H})}$ is the difference between a given band and the uracil monomer N_3H stretch.

of the N_1H and N_3H stretches are equivalent. Further theoretical studies are needed to refine the assignment of these interesting bands.

Uracil–Water Clusters. Mixed uracil–water clusters were generated by bubbling the He carrier gas through a stainless steel reservoir filled with water. All of the other experimental parameters were the same as described in the previous section. The results of the IR-CRLAS scans are shown in Figure 4. This figure also includes a reproduction of the pure uracil scan to demonstrate the location of the new uracil–water bands.

Five new bands, denoted **UW1–5**, are observed and assigned to uracil–water complexes. Three of these bands are relatively narrow (fwhm $\approx 15 \text{ cm}^{-1}$) whereas bands **UW4** and **UW5** are significantly broader and are certainly a convolution of multiple bands. These results are summarized in Table 2. Also included in Table 2 are the differences of the individual bands and the uracil monomer N_3H stretch. Calculated vibrational frequency band positions for uracil–water dimers are given in Table 3,

TABLE 3: Calculated Harmonic Frequency Positions (Unscaled) of Selected Vibrational Modes of Four Uracil–Water Dimers^a

mode	wavenumber	intensity	$\Delta_{(N3H)}$	mode	wavenumber	intensity	$\Delta_{(N3H)}$
Uracil–H ₂ O min 1 $D_e = 42.72$ kJ/mol				Uracil–H ₂ O min 2 $D_e = 34.33$ kJ/mol			
free OH	3690.4	104		free OH	3691.8	101	
free NH	3422.1	69		free NH	3476.3	113	
bonded OH	3322.1	884	205.9	bonded OH	3366.6	553	161.4
bonded NH	3155.9	382	372.1	bonded NH	3148.3	373	379.7
Uracil–H ₂ O min 3 $D_e = 36.03$ kJ/mol				Uracil–H ₂ O min 4 $D_e = 27.43$ kJ/mol			
free OH	3690.2	99		free OH	3705.2	105	
free NH	3471.3	114		free NH	3471.6	115	
bonded OH	3326.1	728	201.9	free NH	3421.4	66	
bonded NH	3122.2	324	405.8	bonded OH	3402.7	585	125.3

^a The D_e are calculated from fully optimized structures using MP2/DZPi.

TABLE 4: Calculated Harmonic Frequency Positions (Unscaled) of Selected Vibrational Modes of Uracil–Water Trimers and Uracil–Water Tetramers^a

mode	wavenumber	intensity	$\Delta_{(N3H)}$	mode	wavenumber	intensity	$\Delta_{(N3H)}$
Uracil(H ₂ O) ₂ min 11 $D_e = 88.78$ kJ/mol				Uracil(H ₂ O) ₂ min 13 $D_e = 79.65$ kJ/mol			
free OH	3685.1	117.7193		free OH	3689.7	53.5575	
free OH	3677.1	71.3581		free OH	3689.3	149.7099	
free NH	3422.3	68.8659		bonded OH	3320.3	539.8738	207.7
bonded OH	3232.3	1551.4563	295.7	bonded OH	3308.0	1132.274	220
bonded OH	3127.6	841.6128	400.4	bonded NH	3142.0	383.6732	386
bonded NH	2846.9	1294.7764	681.1	bonded NH	3110.6	376.4324	417.4
Uracil(H ₂ O) ₂ min 33 $D_e = 77.82$ kJ/mol				Uracil(H ₂ O) ₃ min 113 $D_e = 125.75$ kJ/mol			
free OH	3685.3	76.3936		free OH	3690.0	99.589	
free OH	3684.0	119.2183		free OH	3685.7	113.7838	
free NH	3470.9	109.2372		free OH	3676.4	71.2482	
bonded OH	3257.4	1527.5653	270.6	bonded OH	3310.4	776.5913	271.6
bonded OH	3138.3	787.6749	389.7	bonded OH	3224.4	1544.771	303.6
bonded NH	2772.7	1264.0548	755.3	bonded OH	3148.0	277.4641	380
Uracil(H ₂ O) ₃ min 111 $D_e = 119.62$ kJ/mol				bonded NH	3050.0	1245.25	478
free OH	3688.3	71.3153		bonded NH	2834.3	1366.416	693.7
free OH	3685.1	137.5234					
bonded OH	3550.9	194.6027					
free NH	3422.6	67.2661					
bonded OH	3374.9	583.5063	153.1				
bonded OH	3300.8	313.1867	227.2				
bonded OH	3121.5	1933.1832	406.5				
bonded NH	2722.3	1884.7836	805.7				

^a The D_e are calculated from fully optimized structures using MP2/DZPi.

and those of selected trimers and tetramers previously studied via diffusion quantum Monte Carlo¹² and MP2¹³ are given in Table 4.

In all four uracil–water dimer structures, the water molecule acts both as a hydrogen bond donor and acceptor. Of these, minimum 4 is the only structure wherein a CH hydrogen is involved in hydrogen bonding, and, not surprisingly, it is the least stable structure. On the basis of the calculated band positions and previous matrix work,³¹ we assign bands **UW1**, **UW2**, and **UW3** to the OH stretch of uracil–water dimer clusters. The Ar matrix spectra revealed three red shifted bands at 3431, 3292, and 3276 cm⁻¹, in excellent agreement with the IR–CRLAS results presented here. However, Graindourze et al. assign all bands to “open” dimers, wherein a single hydrogen bond is formed between uracil and water. The main reason for this conclusion was the observation of a splitting of the free NH stretch bands, which they interpreted as evidence of a weak secondary perturbation of the NH bond vicinal to the CO group hydrogen bonded to the water molecule. However, those split NH bands were approximately five times stronger than the red-shifted OH bands. Clearly, this assignment needs to be revised, as the bonded OH stretch bands should be significantly stronger than any free NH band. In fact, given the signal-to-noise ratio

of their bonded OH stretch bands, any free NH stretch bands due to uracil–water clusters would be below their detection limit. Finally, the calculations by van Mourik et al. show that single hydrogen-bonded structures are actually transition states on the uracil–water dimer PES.¹²

The fact that we only observe three dimer OH stretch bands indicates that only three uracil–water isomers are present in the molecular beam. Comparison between the IR–CRLAS results and the ab initio calculations (see the $\Delta_{(N3H)}$ column in Tables 4.2 and 4.3) suggests that the clusters present in the expansion are minima 1, 3, and 4. This result is in agreement with the OPLS DMC calculations, which show that minimum 2 is not vibrationally stable (it interconverts to minimum 3). However, van Mourik et al. found that the OPLS potential significantly underestimates the barrier height to interconversion.¹² As was mentioned previously, the authors found that all minima are vibrationally stable when studied at the MP2/DZPi level of theory. As a result, we assign bands **UW1**, **UW2**, and **UW3** to structures 2, 3, and 1, respectively. The agreement between **UW1** and the calculated hydrogen-bonded OH stretch frequency of structure 2 is not very good, but given the fact that all minima are vibrationally stable, it is unlikely that minima 4 is present in the expansion and minima 2 is not. This is further supported

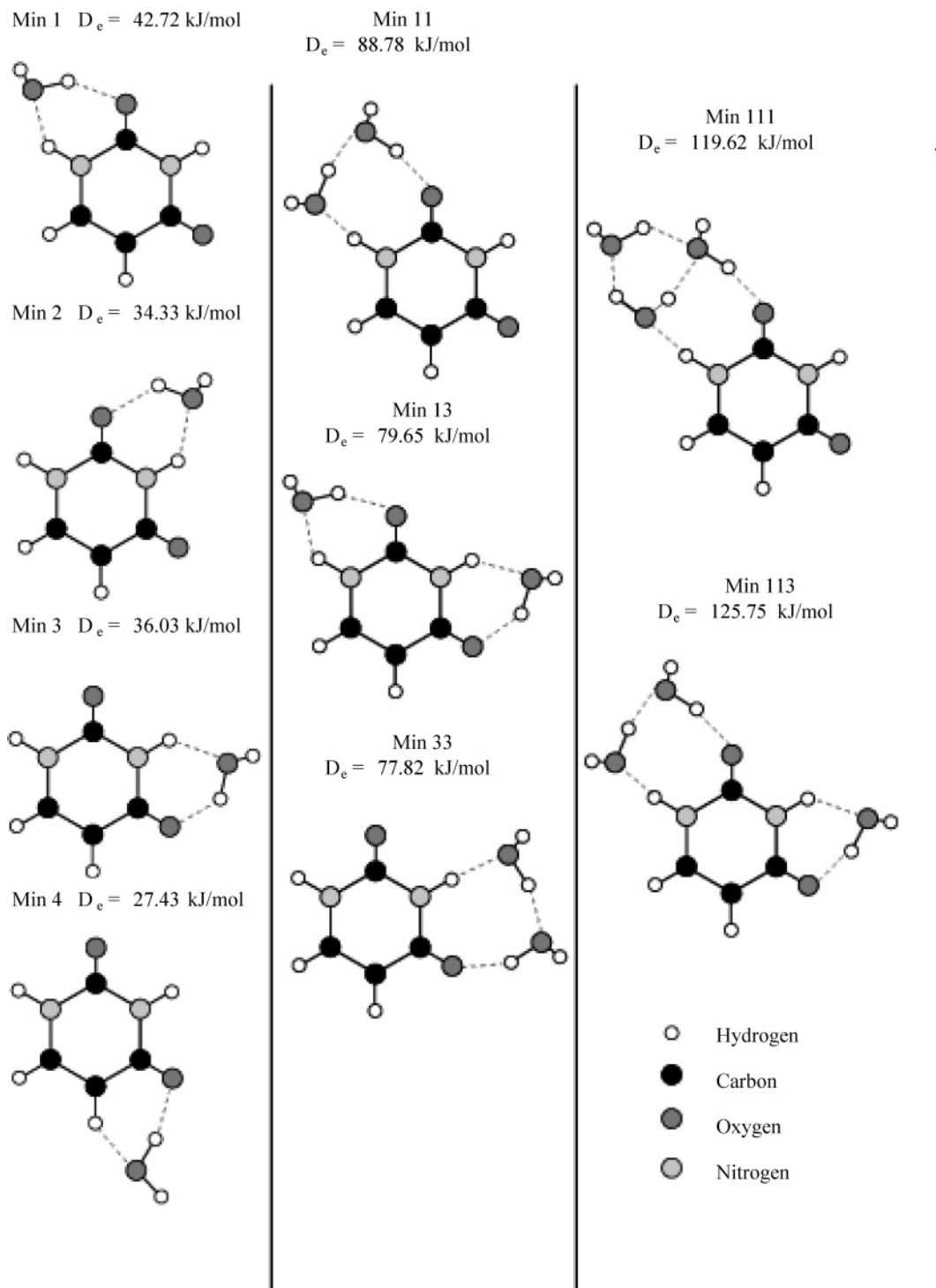


Figure 5. Calculated structures of uracil–water clusters from ref 12 and 13. All of the clusters were optimized with MP2/DZPi.

by the uracil cluster work, wherein no evidence was found for the presence of a uracil dimer cluster with a CH hydrogen bond.

The frequency of the **UW4** band centered at 3181 cm^{-1} is in excellent agreement with the calculated bonded NH stretches of uracil–water dimers. However, the bonded NH stretches are significantly weaker than the bonded OH stretches, although band **UW4** is approximately two times stronger than bands **UW1–3**. Furthermore, band **UW5** cannot be assigned to any of the dimer structures. As a result, the theoretical results imply that clusters larger than the dimer must be present in the expansion. Table 4 shows the calculated harmonic frequency positions of selected vibrational modes for three trimer structures and two tetramer structures shown in Figure 5.

Because bands **UW4** and **UW5** are broad, indicating that they are a convolution of several bands, and the current experiment does not have mass selection to differentiate between band carriers as a function of cluster size, all of the subsequent assignments are tentative. On the basis of the theoretical results, we assign band **UW4** to a convolution of the bonded NH stretches of the uracil–water dimers 1, 2, 3, and the bonded OH stretches of the uracil–water trimers 11 and 33. We see no evidence for the presence of the uracil–water trimer 13, as this cluster should have two strong bands, with intensity ratios of 2:1, to the blue of band **UW4**. This leaves the other two bonded OH stretches of structures 11 and 33 as possible carriers of and **UW5**. However, the theoretical calculations predict that the bluer

TABLE 5: Assignment of the Uracil–Water IR-CRLAS Data

band	assignment
UW1	bonded NH stretch U(H ₂ O) min 2
UW2	bonded NH stretch U(H ₂ O) min 3
UW3	bonded NH stretch U(H ₂ O) min 1
UW4	bonded NH stretch U(H ₂ O) min 1, 2, 3 bonded OH stretch U(H ₂ O) ₂ min 11, 33 bonded OH stretch U(H ₂ O) ₃ min 113
UW5	bonded OH stretch U(H ₂ O) ₂ min 11, 33 bonded OH stretch U(H ₂ O) ₃ min 111 bonded NH stretch U(H ₂ O) ₃ min 113

OH stretches of structures 11 and 33 are approximately two times stronger than the corresponding redder OH stretches, whereas band **UW5** is stronger than band **UW4**. As a result, band **UW5** must also include contributions from a bonded OH stretch of tetramer 111 and a bonded NH stretch of tetramer 113. These assignments are summarized in Table 5.

The IR-CRLAS results confirm the unusually large bonded OH stretch red shifts predicted by ab initio calculations. The measured bonded OH stretch red shifts of uracil–water dimers are approximately 250 cm⁻¹ greater than the corresponding bonded OH stretch red shift of the water trimer and 150 cm⁻¹ greater than the bonded OH stretch red shift of the water tetramer.²⁸ These large red shifts are indicative of extremely strong hydrogen bonds formed between water and uracil. Perhaps the most surprising aspect of the IR-CRLAS data is the absence of bands due to pure water clusters. Several pure water clusters, the tetramer, pentamer, and hexamer, have OH stretch bands in this region. Furthermore, under source conditions similar to those employed here but without uracil in the expansion, the source produces large water clusters characterized by a broad and very intense band (>1000 ppm) centered around 3250 cm⁻¹.²⁸ Even though the uracil–water interaction is favored over water–water interactions, as shown by Gadre et al.,⁹ it was expected that pure water clusters would form simply due to the greater number density of water molecules in the expansion. The absence of pure water cluster bands indicates that any small water cluster formed in the expansion subsequently complexes with uracil monomers or small uracil–water clusters.

Conclusions

We have measured the gas-phase infrared spectra of jet-cooled uracil clusters, thymine clusters, and uracil–water mixed clusters in the NH and OH stretch regions. The uracil and thymine data indicate the presence of several different clusters in the molecular beam. Evidence is given for the presence of several double hydrogen-bonded uracil dimer clusters, but no singly hydrogen bonded clusters, and for the formation of a larger highly symmetrical cluster.

The uracil–water data indicate the presence of three dimer isomers as well as several trimer and tetramer clusters. Because of significant band overlap, assignment of the bands to specific trimer and tetramer isomers is tentative. Extremely large red shifts are observed for all of the clusters studied here, in agreement with ab initio calculations, indicating the presence of very strong hydrogen bonds.

Acknowledgment. This work was supported by the Experimental Physical Chemistry Program of the NSF and the Chemical Dynamics Program of the AFOSR.

References and Notes

- (1) Gueron, M.; Kochoyan, M.; Leroy, J. L. *Nature* **1987**, *328*, 89–92.
- (2) Spomer, J.; Leszczynski, J.; Hobza, P. *J. Phys. Chem.* **1996**, *100*, 5590–5596.
- (3) Kratochvil, M.; Engkvist, O.; Spomer, J.; Jungwirth, P.; Hobza, P. *J. Phys. Chem. A* **1998**, *102*, 6921–6926.
- (4) Hobza, P.; Spomer, J.; Cubero, E.; Orozco, M.; Luque, F. J. *J. Phys. Chem. B* **2000**, *104*, 6286–6292.
- (5) Leininger, M. L.; Nielsen, I. M. B.; Colvin, M. E.; Janssen, C. L. *J. Phys. Chem. A* **2002**, *106*, 3850–3854.
- (6) Ilich, P.; Hemann, C. F.; Hille, R. *J. Phys. Chem. B* **1997**, *101*, 10923–10938.
- (7) van Mourik, T.; Price, S. L.; Clary, D. C. *J. Phys. Chem. A* **1999**, *103*, 1611–1618.
- (8) Dolgounitcheva, O.; Zakrzewski, V. G.; Ortiz, J. V. *J. Phys. Chem. A* **1999**, *103*, 7912–7917.
- (9) Gadre, S. R.; Babu, K.; Rendell, A. P. *J. Phys. Chem. A* **2000**, *104*, 8976–8982.
- (10) Gaigeot, M. P.; Kadri, C.; Ghomi, M. *J. Mol. Struct.* **2001**, *565*, 469–473.
- (11) van Mourik, T.; Benoit, D. M.; Price, S. L.; Clary, D. C. *Phys. Chem. Chem. Phys.* **2000**, *2*, 1281–1290.
- (12) van Mourik, T.; Price, S.; Clary, D. *Faraday Discuss.* **2001**, *118*, 95–108.
- (13) van Mourik, T. *Phys. Chem. Chem. Phys.* **2001**, *3*, 2886–2892.
- (14) Szczesniak, M.; Nowak, M.; Rostkowska, H.; Szczepaniak, K.; Person, W.; Shugar, D. *J. Am. Chem. Soc.* **1983**, *105*, 5969.
- (15) Chin, S.; Scott, I.; Szczepaniak, K.; Person, W. *J. Am. Chem. Soc.* **1984**, *106*, 3415.
- (16) Barnes, A.; Stuckey, M.; Gall, L. L. *Spectrochim. Acta, Part A* **1984**, *40*, 419.
- (17) Graindourze, M.; Smets, J.; Zeegers-Huyskens, T.; Maes, G. *J. Mol. Struct.* **1990**, *222*, 345–364.
- (18) Les, A.; Adamowicz, L.; Nowak, M.; Lapinski, L. *Spectrochim. Acta, Part A* **1992**, *48*, 1385.
- (19) Ivanov, A. Y.; Plokhotnichenko, A. M.; Radchenko, E. D.; Sheina, G. G.; Blagoi, Y. P. *J. Mol. Struct.* **1995**, *372*, 91–100.
- (20) Colarusso, P.; Zhang, K. Q.; Guo, B. J.; Bernath, P. F. *Chem. Phys. Lett.* **1997**, *269*, 39–48.
- (21) Maes, G.; Graindourze, M.; Smets, J. *J. Mol. Struct.* **1991**, *248*, 89–110.
- (22) Brady, B.; Peteanu, L.; Levy, D. *Chem. Phys. Lett.* **1988**, *147*, 538–543.
- (23) Desfrancois, C.; Periquet, V.; Bouteiller, Y.; Schermann, J. *J. Phys. Chem. A* **1998**, *102*, 1274–1278.
- (24) Schiedt, J.; Weinkauff, R.; Neumark, D. M.; Schlag, E. W. *Chem. Phys.* **1998**, *239*, 511–524.
- (25) Viant, M.; Fellers, R.; McLaughlin, R.; Saykally, R. *J. Chem. Phys.* **1995**, *103*, 9502.
- (26) Keutsch, F.; Saykally, R. *Proc. Natl. Acad. Sci. U.S.A.* **2001**, *98*, 10533–10540.
- (27) Paul, J. B.; Saykally, R. *J. Anal. Chem.* **1997**, *69*, 287–292.
- (28) Paul, J. B.; Collier, C. P.; Saykally, R. J.; Scherer, J. J.; O’Keefe, A. *J. Phys. Chem. A* **1997**, *101*, 5211–14.
- (29) Liu, K.; Fellers, R. S.; Viant, M. R.; McLaughlin, R. P.; Brown, M. G.; Saykally, R. *J. Rev. Sci. Instrum.* **1996**, *67*, 410–416.
- (30) Chapo, C. J.; Paul, J. B.; Provencal, R. A.; Saykally, R. J. *J. Am. Chem. Soc.* **1998**, *120*, 12956.
- (31) van Mourik, T. Ph.D. Thesis, University Utrecht, 1994.
- (32) van Mourik, T.; Price, S. L.; Clary, D. C. *Chem. Phys. Lett.* **2000**, *331*, 253.
- (33) Bowman, J. M. *J. Chem. Phys.* **1978**, *68*, 608.
- (34) Gerber, R. B.; Chaban, G. M.; Gregurick, S. K.; Brauer, B. *Biopolymers* **2003**, *68*, 370.
- (35) Benoit, D. M. *J. Chem. Phys.* **2004**, *120*, 562.
- (36) Scott, A. P.; Radom, L. *J. Phys. Chem.* **1996**, *100*, 16502.
- (37) Schoone, K.; Smets, J.; Ramaekers, R.; Houben, L.; Adamowicz, L.; Maes, G. *J. Mol. Struct.* **2003**, *649*, 61.
- (38) Ramaekers, R.; Houben, L.; Adamowicz, L.; Maes, G. *Vib. Spectrosc.* **2003**, *32*, 185.
- (39) van Mourik, T. Unpublished work.
- (40) Graindourze, M.; Grootaers, T.; Smets, J.; Zeegers-Huyskens, T.; Maes, G. *J. Mol. Struct.* **1991**, *243*, 37–60.